

Temperature-Dependent Transport Properties of Poly[2-(methacryloyloxy)ethyl]trimethylammonium Chloride Brushes Resulting from Ion Specific Effects

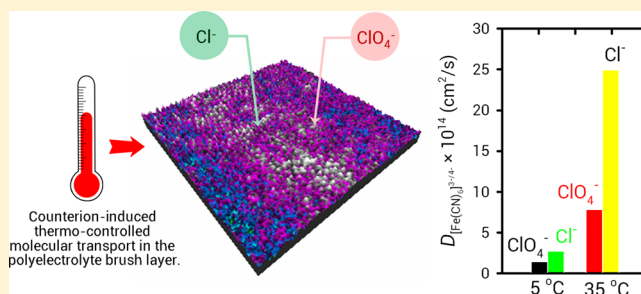
Teodoro Alonso-García,[†] Claudio A. Gervasi,^{*,‡,§} María José Rodríguez-Presa,[‡] Eduart Gutiérrez-Pineda,^{‡,§} Sergio E. Moya,[†] and Omar Azzaroni^{*,‡}

[†]Biosurfaces Unit, CIC biomaGUNE, Paseo Miramón 182 C, 20009 San Sebastián, Gipuzkoa, Spain

[‡]Facultad de Ciencias Exactas, Instituto de Investigaciones Fisicoquímicas Teóricas y Aplicadas (INIFTA), UNLP-CONICET, Sucursal 4-C.C. 16, 1900 La Plata, Argentina

[§]Facultad de Ingeniería, Laboratorio de Ingeniería de Corrosión y Tecnología Electroquímica, LICTE, UNLP, 1 y 47, 1900, La Plata, Argentina

ABSTRACT: Combined use of electrochemical techniques (electrochemical impedance spectroscopy and cyclic voltammetry) and quartz crystal microbalance with dissipation allowed to resolve separately the thermal effects on diffusion and electron-transfer steps of the electrochemical reaction of the $[\text{Fe}(\text{CN})_6]^{3-/4-}$ redox couple at a Au electrode modified with poly[2-(methacryloyloxy)ethyl]trimethylammonium chloride (PMETAC) brushes. Arrhenius-type dependences of the kinetic constant and the diffusion coefficient with temperature were observed in different electrolytes. Ion-paired collapsed polyelectrolyte brushes in NaClO_4 result in compact stiff structures with less amount of entrapped water and markedly different from the same brushes with a collapse driven by pure Coulombic screening in NaCl . A remarkable difference related to the type of counterion is the occurrence of a thermal transition for the polyelectrolyte brush in the presence of ClO_4^- ions at near-ambient temperature ($\sim 17^\circ\text{C}$). Activation energies for electron-transfer and diffusion processes become twice as large as those for temperatures above the thermal transition. These electrochemical studies demonstrate not only the critical role of ion-pairing interactions in determining the physicochemical properties of the macromolecular system but also provide experimental evidence of counterion-induced thermocontrolled transport functionality in the polyelectrolyte brush layer.



1. INTRODUCTION

Polyelectrolyte (PE) brushes are assemblies of charged macromolecules tethered at one end of their chains to a substrate while the other end is free. PE brushes normally exhibit a responsive behavior (transition between extended and collapsed conformational states) with changes in the ionic strength of the solution inside the polymer matrix. Thus, brush thickness, mechanical properties, friction, and wettability can be varied by changing the ionic strength and in some cases by means of specific ion interactions, i.e., the so-called hydrophobic or ion-pairing collapse. This responsive character of PE brushes has been explored in the design of surfaces with a “smart” function.¹

Poly[2-(methacryloyloxy)ethyl]trimethylammonium chloride (PMETAC) brushes are cationic PE brushes that have been shown to suffer a hydrophobic collapse as mentioned above.² This hydrophobic collapse is explained as a result of a strong interaction between the quaternary ammonium groups of the brushes with large polarizable ions such as ClO_4^- or I^- . These ions have affinity for unstructured water and find a suitable environment in the bulky hydrophobic region of the

quaternary ammonium groups, contributing at the same time to an increase in their hydrophobic character. As a consequence, brush collapse in presence of these ions takes place at lower counterion concentrations than when collapse is driven purely by changes in the solution ionic strength, e.g., in the presence of NaCl . Moreover, the hydrophobic collapse results in a much larger water loss for the brush and induces a significant change in surface wettability. The percentage of water removed reaches ca. 54% in 0.1 M ClO_4^- in contrast to slightly more than 17% in 0.1 M Cl^- solution.^{3,4}

Among the different properties of the brush that are affected by the brush collapse, the transport properties are of particular importance since they are essential for the application of brushes as coating or barriers. It has been indeed shown how the swelling/collapse behavior of thin polyelectrolyte brushes governs the interfacial impedance.^{5,6} Transport phenomena have been recently studied by impedance methods in PMETAC

Received: October 14, 2013

Revised: December 2, 2013

Published: December 11, 2013

brushes under collapse due to both pure charge screening and ion pairing, in the presence of NaCl and NaClO₄, respectively.⁷ Results obtained at 25 °C show that the diffusion of an electroactive probe is significantly restricted inside the brush in both electrolytes with diffusion coefficient values ranging from 2×10^{-13} to 5×10^{-14} cm² s⁻¹. Clearly, differences in probe mobility between both electrolytes are relatively small at 25 °C. Slightly lower diffusion coefficients measured in NaClO₄ solution as compared with NaCl solution can be understood on the basis of the lower water content that restricts the diffusive pathways of the probe within the brush and limits polymer chain mobility of the brushes.

Recently we have also shown that measuring the electrochemical behavior of PMETAC brushes in presence of ClO₄⁻ ions a steep thermal transition at 17 °C can be observed for the brushes. In this work we aim at addressing the activity of the brush-modified electrode according to the temperature and in relation to the nature of the counterion and the type of collapse associated with the brushes, either by Coulombic screening or ion-pairing interactions. By doing so, we intend to obtain a deeper insight into the brush structure during the collapse. Transport studies according to the temperature are also fundamental for the application of brushes as barriers or for permeability control. Moreover, the study of transport phenomena in relation to the temperature can provide fundamental information to interrogate the mechanisms of diffusion of electroactive probes through brushes. Indeed, an electrochemical reaction on the surface of an electrode has two limiting mechanisms: the reaction is under kinetic control or the reaction is controlled by the diffusion of the electroactive species. Recently, in order to describe the electrochemical response of the modified electrode a model was presented considering a planar diffusion step for an electroactive molecular probe, where the brush layer acts as a diffusion-limiting barrier of finite thickness, followed by the electron-transfer step at the electrode surface.⁷ In these studies, it was shown that the conformational transition of the polymer brush affects the mass transport of the redox probe through the new structure of the macromolecular array and, for a strongly collapsed brush, this also affects the fraction of active surface available for the electron transfer. Since both diffusion and electron transfer are activated processes, but only the electron-transfer rate is dependent on the active surface (unlike the diffusion coefficient), a study of the temperature dependence of the rate constant and the diffusion coefficient allows us to deepen our understanding on this subject. Therefore, in a scenario of a possible temperature-affected characteristic for this interface it is essential to assess whether the polymer brush suffering a transition process preferentially restricts mass transport or blocks electron transfer at the active electrode surface. Additionally, quantifying temperature effects on both the diffusion coefficient and the rate constant represents a useful way to validate the proposed theoretical model and derive useful thermodynamic data to get an insight as to how the relative contributions of each reaction step determine the reaction control according to the brush conformational state.

In the present article the interfacial electrochemical behavior of Au electrodes modified with PMETAC brushes was characterized varying bulk temperature in 0.1 M NaCl and NaClO₄ solutions by electrochemical impedance spectroscopy (EIS) and cyclic voltammetry (CV) using [Fe(CN)₆]^{3-/4-} as the redox probe. Additionally, quartz crystal microbalance with dissipation (QCM-D) studies were performed to assess changes

in brush thickness and water content with the different salts studied.

2. EXPERIMENTAL SECTION

2.1. Synthesis of Polyelectrolyte Brushes. PE brushes were grown from self-assembled monolayers (SAMs) of ω -mercaptoundecylbromobutyrate as the initiator thiol. The thiol monolayers were deposited on clean gold substrates whose preparation is described in detail elsewhere.⁸ The assembly of the thiol was performed from a 10⁻² M methanolic solution of the initiator. Brushes were synthesized by atom-transfer radical polymerization (ATRP). The polymerization solution was prepared as follows: 1 mL of commercially available (Aldrich) METAC monomer (75 wt % solution in water), 40 mmol, was dissolved in a mixture of 2 cm³ of water and 3 cm³ of dimethylformamide (DMF), 99.85%, at 20 °C and degassed by passing a continuous stream of dry N₂ through the solution while being stirred, approximately for 15 min. 2,2'-Bipyridyl (416 mg, 2.7 mmol), Cu^ICl (105 mg, 1.1 mmol), and Cu^{II}Cl₂ (14 mg, 0.11 mmol) were added to this solution. The mixture was then further stirred and degassed with a stream of dry N₂ for another 15 min. Gold substrates coated with the initiator were sealed in Schlenk tubes, degassed, and left at 20 °C under N₂. The polymerization solution was then syringed into each Schlenk tube, adding enough solution to submerge each sample completely. Once the polymerization step is accomplished, the samples were carefully removed from the Schlenk tubes, washed with water and then with methanol, and finally dried under a stream of N₂.

2.2. Characterization Techniques. *In Situ* QCM-D Measurements. Growth of the polymer brush and brush thickness were measured by QCM-D on the same surface and in the same liquid environment. Measurements were performed using a purpose-built flow cell (Q-Sense AB, Västra Frölunda, Sweden) with a total volume of ~300 μ L. The flow cell was attached to a Q-Sense E1 setup, providing access to QCM-D data. QCM-D data, Δf and ΔD , were acquired at six overtones ($i = 3, 5, \dots, 13$, corresponding to resonance frequencies of $f_i \approx 15, 25, \dots, 65$ MHz) simultaneously, with subsecond time resolution.

Electrochemical Techniques. Electrochemical measurements were carried out within the 5–45 °C temperature range in a conventional three-electrode cell. A platinum sheet with large area and a saturated calomel electrode (SCE) were used as the counter electrode and the reference electrode, respectively. All potentials are referred to the SCE at 25 °C. Au substrates coated with brushes served as working electrodes. Solutions of 0.1 M NaCl and 0.1 M NaClO₄ were used as supporting electrolytes and prepared from analytical grade (Merck) reagents and Milli-Q water. Experiments were performed under purified N₂ gas saturation in a solution of the redox couple consisting of 1 mM K₃[Fe(CN)₆]/K₄[Fe(CN)₆] (1:1) mixture in the supporting electrolytes. As already discussed by Huck and co-workers, due to their much larger concentration, counterions will preferentially displace redox probe molecules coordinated with PMETAC brush chains, and consequently, conformational collapse of PMETAC brushes proceeds only affected by the presence of chloride and perchlorate ions.⁹ CV measurements were performed by scanning the potential at a scan rate of 0.05 V s⁻¹.

Impedance spectra were obtained with a Zahner IM6d electrochemical workstation. The dc potential of the working electrodes was held at the open circuit potential while a 10 mV

amplitude ac potential was applied. The voltage signal frequencies used for EIS measurements ranged from 100 kHz to 1 MHz. Impedance data analysis was performed according to proper procedures for transfer function derivation and identification by using complex nonlinear least-squares (CNLS) fitting based on the Marquardt–Levenberg algorithm.

3. RESULTS AND DISCUSSION

Figure 1 shows data recorded with the QCM-D technique as the third overtone evolution with time of the acoustic

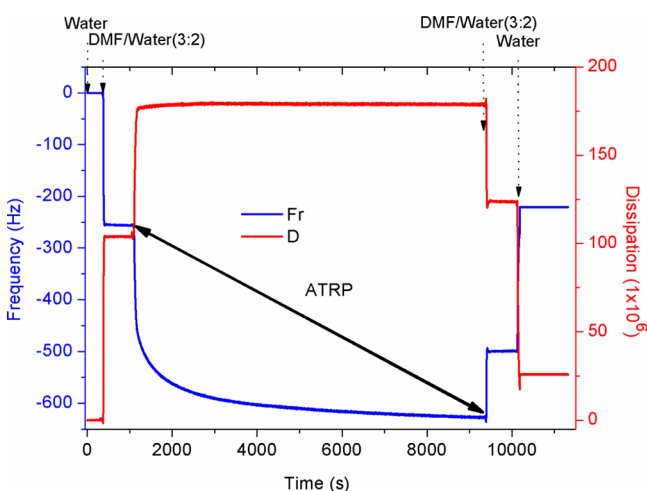


Figure 1. Synthesis of the PMETAC brush from a monolayer of ω -mercaptoundecylbromobutyrate assembled on top of a gold surface. QCM-D response, i.e., Δf and ΔD vs time for a selected overtone (third).

parameters frequency (blue line) and dissipation (red trace) related to the growth of a PMETAC brush grown from a monolayer of ω -mercaptoundecylbromobutyrate previously assembled on the gold-coated QCM-D substrate. Frequency follows a continuous decrease according to the polymerization process; that is indicative of the progressive mass growth on top of the substrate. At the same time, values for the dissipation rise as the polymerization progresses, indicating the formation of a film with a viscoelastic character. After ATRP polymerization, a consecutive rinse with a DMF/water (3:2) mixture and pure water sweeps the polymerization solution away. This results in an increase in frequency and a corresponding decrease in dissipation. Considering the relationship between dissipation and frequency values and the Sauerbrey equation (see below), it is possible to estimate the increase in total film mass, m_{QCM} , as the brush grows according to the total measured change in frequency $\Delta f = -225$ Hz.

Figure 2 shows the time evolution of frequency and dissipation (third overtone) during a brush collapse in presence of 0.1 M NaCl. The salt solution was injected at minute 10, causing an increase in the frequency in 30 Hz and a decrease in dissipation in 14 relative units.

Figure 3 depicts time evolutions of frequency and dissipation (third overtone). Larger values for the changes in the acoustic parameters associated with a brush collapse due to the addition of 0.1 M NaClO₄ indicate a stronger effect of perchlorate ion in comparison with chloride ion.

QCM-D data were evaluated quantitatively in terms of the Sauerbrey equation that links frequency shifts and adsorbed masses per unit area in the following simple way:¹⁰

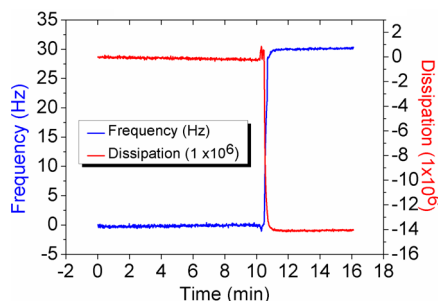


Figure 2. Temporal variation of the frequency (blue line) and dissipation (red trace) during the collapse of the PMETAC brush in 0.1 M NaCl solution.

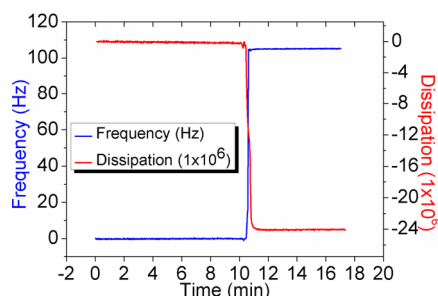


Figure 3. Temporal variation of frequency (blue line) and dissipation (red trace) related to a PMETAC brush collapse in 0.1 M NaClO₄ solution.

$$m_{\text{QCM}} = -C \frac{\Delta f_i}{i} \quad (1)$$

with the mass sensitivity constant, $C = 18.06 \pm 0.15$ ng·cm⁻²·Hz⁻¹ for sensors with a resonance frequency of 4.95 ± 0.02 MHz, and the overtone number i . The normalized frequency shifts, $\Delta f = \Delta f_i/i$, for the third overtone were employed to determine m_{QCM} . The applicability of eq 1 is limited to sufficiently rigid films. For soft and dissipative films, more complex models would be required that account for their viscoelastic properties.^{11,12}

For the PMETAC brushes investigated here, the ratio of dissipation and normalized frequency shifts, $\Delta D/(-\Delta f)$, indicates that eq 1 is a good approximation. The application of different viscoelastic models to selected data sets (details of the modeling procedure are given elsewhere¹³) corroborated that the Sauerbrey equation is indeed a good approximation for our films, with an error below 5%. The experimental noise was typically below 2 ng/cm².

The brush thickness was further determined by

$$d_{\text{QCM}} = m_{\text{QCM}}/\rho_{\text{brush}} \quad (2)$$

where $\rho_{\text{brush}} = 1.0$ g/cm³ is the density of the solvated polymer film. In the pure form, the employed polymer exhibits densities between 1.0 and 1.1 g/cm³, while the density of water or salt solutions is also 1.0 g/cm³. Hence, eq 2 could overestimate the thickness by at most 10%.

Combining eqs 1 and 2 results in the following relationship: $d_{\text{QCM}}/\text{nm} \cong -1/5 \Delta(f/\text{Hz})$ that relates film thicknesses and the corresponding normalized frequency shifts at the end of the polymerization step (brush immersed in water) and after exposure of the brushes to the salt solutions (0.1 M NaCl and 0.1 M NaClO₄), respectively.

Owing to its acoustomechanical transducer principle, the QCM-D technique is not only sensitive to the adsorbed molecules but also to the solvent retained within or hydrodynamically coupled to the surface-bound film. Therefore, from the QCM frequency response alone, it is difficult to discriminate between the adsorbed polymer mass and the contribution of the solvent coupled to the polymer. Polyelectrolytes are charged molecules with hydrated monomers. Besides that, water can be entrapped in cavities between neighboring chains. The QCM-D will thus sense the total mass of the brush, consisting of polyelectrolyte and water. Moreover, it can measure the amount of water that is reversibly lost during collapse with the ionic strength.⁴

An evaluation of data in Figure 1 yields $\Delta f = -225$ Hz, corresponding to $d_{\text{QCM}} = 45$ nm. This value represents the total thickness in aqueous medium of the PMETAC brush.

From Figure 2 a change $\Delta f = 30$ Hz can be observed after adding 0.1 M NaCl corresponding to a reduction in film thickness of 6 nm, while the addition of 0.1 M NaClO₄ results in a Δf change = 105 Hz, corresponding to a reduction in film thickness of 21 nm. Consequently, final thicknesses of collapsed PMETAC brushes are 39 nm in 0.1 M NaCl solution and 24 nm in 0.1 M NaClO₄ solution, as shown in Figure 4.

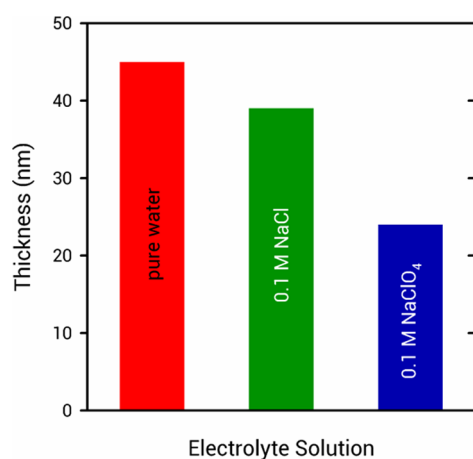


Figure 4. Calculated values for the acoustic thickness (d_{QCM}) as measured in pure water, chloride, and perchlorate solutions.

Exposure of the brush to salt solutions yielded positive changes in frequency, indicative of brush collapse and water mass loss.¹⁴ Data from the literature inform the hydration percentage of PMETAC brushes in water and after collapse transitions in Cl⁻ and ClO₄⁻-containing electrolytes.^{4,15} The initial water content of the brushes, expressed as the percentage of solvent contributing to the total film mass, was informed to be ca. 67%. Comparing the percentages of water loss related to collapsed conditions it can be observed that while NaCl solution only removes 17% of the entrapped water through the originated collapse, NaClO₄ solution provokes the release of 54% of the water initially entrapped before collapse.

In Figure 5 we observe the effect of changing the electrolyte temperature T on the voltammetric response of an electrode modified with a PMETAC brush in 0.1 M Cl⁻ solution containing 1 mM K₃[Fe(CN)₆]/K₄[Fe(CN)₆].

Comparable results are shown in Figure 6 for the same experimental conditions as in Figure 5 but in 0.1 M ClO₄⁻ solution containing 1 mM K₃[Fe(CN)₆]/K₄[Fe(CN)₆].

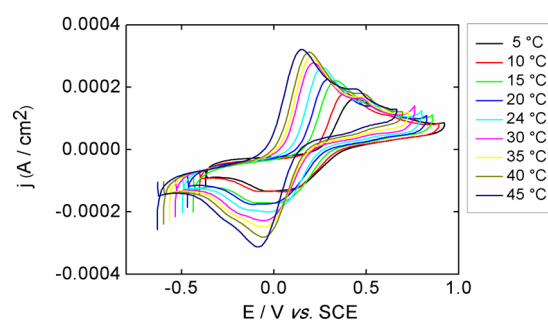


Figure 5. Voltammetric responses of a brush-modified Au electrode in 0.1 M NaCl + 1 mM [Fe(CN)₆]^{3-/4-} for different electrolyte temperatures as indicated in the inset.

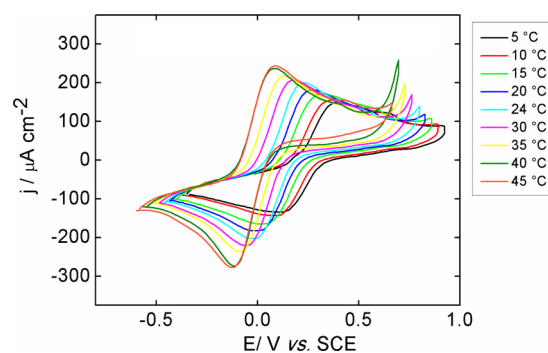


Figure 6. Voltammetric response of a Au electrode coated with a PMETAC brush in 0.1 M NaClO₄ + 1 mM [Fe(CN)₆]^{3-/4-} at different electrolyte temperatures as indicated in the inset.

Anodic and cathodic peak current densities j_p become larger at higher T in both electrolytic solutions.

The separation of peak potentials (ΔE_p) becomes smaller for higher T , in both electrolytes, as shown in Figure 7, although, at

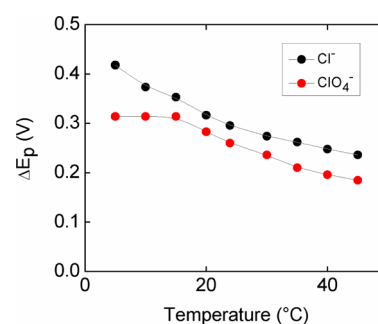


Figure 7. Variation of the separation of peak potentials (ΔE_p) with the electrolyte temperature for chloride and perchlorate solutions. Values derived from data in Figures 5 and 6.

each temperature, ΔE_p is larger than the value obtained for the same redox couple on bare gold surfaces that is characterized by a highly reversible electrochemical reaction. ΔE_p values measured in NaClO₄ solution are almost constant at the lowest studied temperatures; in principle, this indicates a singular behavior associated with the presence of the ClO₄⁻ anion. Here, it is perhaps worth mentioning that voltammetric peaks in the low- T range are less sharp while peak current values cover a somewhat extended potential window. It has been indicated in the literature that it is necessary to be cautious about interpreting these trends because of the

difficulties in determining accurate redox potentials from voltammograms adopting a sigmoidal shape.¹⁶

Data in Figures 5, 6, and 7 are consistent with a quasi-reversible electron-transfer model. For a SAM-modified electrode a marked decrease in the peak currents is observed in the cyclic voltammogram as well as an increase in the splitting of the peak potentials, while the voltammogram tends to adopt a sigmoidal shape. These observations indicate that the electron-transfer reaction might be occurring at pinhole sites.¹⁷

Higher peak current densities and smaller peak separations for increasing T can be interpreted in terms of faster electrochemical kinetics exhibited by the electron-transfer reaction at the surface and higher diffusion coefficients D of the redox probe inside the brush. However, one cannot succeed in separating the individual effects of T on each reaction step from the voltammetric responses. Thus, slow interfacial charge transfer cannot be distinguished from hindered diffusion effects. Therefore, to gain a deeper insight into this question we performed impedance experiments, where both effects can be separated.

Figure 8 shows impedance spectra for an electrode modified with the PMETAC brush immersed in NaCl solution at

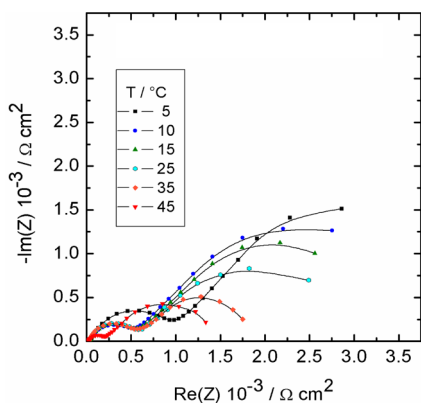


Figure 8. Nyquist plots of the experimental impedance measured with a Au electrode modified with a PMETAC brush at different temperatures in the presence of 1×10^{-3} M $[\text{Fe}(\text{CN})_6]^{3-/4-}$ + 0.1 M NaCl.

different temperatures within the 5–45 °C range. Nyquist diagrams in Figure 9 exhibit a semicircle in the high-frequencies f region followed at low frequencies by impedance values containing diffusion effects corresponding with a finite-length diffusion-type impedance. Impedance values decrease according to T in the whole frequency range.

The same qualitative behavior was measured for an electrode modified with the polyelectrolyte brush immersed in NaClO_4 solution (Figure 9).

The high- f semicircle is related to electron-transfer processes at the uncovered gold surface.¹⁸ The semicircle diameter represents the charge-transfer resistance R_{ct} , whereas the intercept of the semicircle with the real part of the impedance $\text{Re}(Z)$ -axis for $f \rightarrow \infty$ corresponds to the bulk solution resistance, R_e . R_{ct} contains kinetic information according to the following expression.^{6,7}

$$\frac{1}{R_{ct}} = A_e F \left[C_O^{\text{dc}} \left(\frac{k_c \alpha_c F}{RT} \right) + C_R^{\text{dc}} \left(\frac{k_a \alpha_a F}{RT} \right) \right] \quad (3)$$

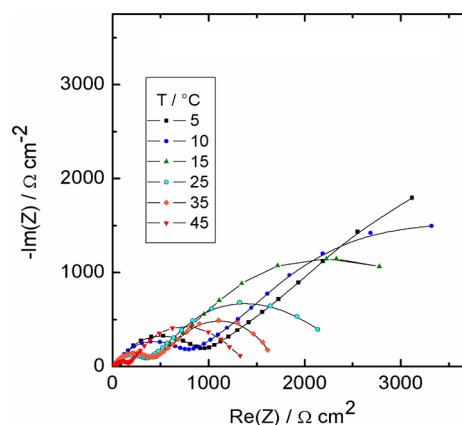


Figure 9. Nyquist plots of the experimental impedance measured with a Au electrode modified with a PMETAC brush at different temperatures in the presence of 1×10^{-3} M $[\text{Fe}(\text{CN})_6]^{3-/4-}$ + 0.1 M NaClO_4 .

where α_a and α_c are the transfer coefficients, k_a and k_c correspond to the rate constants for the anodic and cathodic reactions, respectively, C_O and C_R represent concentrations of the oxidized and reduced species at the surface for dc conditions, and A_e is the electrode area while R and F are the gas and Faraday constants, respectively.

Impedance values in the low- f region are related to the brush layer building a diffusion-limiting barrier of finite thickness δ for the electroactive molecular probes. In this way the electrode is uniformly accessible to mass transfer through a hydrated brush of finite thickness.

In the transition region between the semi-infinite and the true finite diffusion control, where the angular frequency $\omega \approx D/\delta^2$ and the Nernst diffusion layer thickness δ corresponds to the distance traveled by the diffusion species for the low-frequency oscillating perturbations and is equivalent to the brush thickness d . Then, the diffusion impedance Z_d is given by¹⁹

$$Z_d = \frac{\sigma}{\sqrt{\omega}} [\tanh(B\sqrt{i\omega})] (1 - i) \quad (4)$$

where $i = \sqrt{-1}$, $\omega = 2\pi f$ and is the angular frequency of the potential perturbation, the so-called mass-transfer coefficient σ contains the contributions of the oxidized and reduced forms of the redox couple and $B = \delta/\sqrt{D}$. As already indicated above, $\delta = d$, i.e., the thickness of the polymer brush and D is the diffusion coefficient. The complete mathematical treatment used to derive eqs 3 and 4 can be found elsewhere.^{6,7}

Experimental impedance data were fitted to the following theoretical expression for the electrode impedance Z_t :

$$Z_t = R_e + \frac{1}{(i\omega)^n Y_o + \frac{1}{R_{ct} + Z_d}} \quad (5)$$

resulting from the inclusion of a constant phase element of impedance that carries the nonfaradaic portion of the current and contains the parameter Y_o that can be used to derive the interfacial capacitance C_i with the consideration of a distribution of values on the surface. As usual, when the exponent $n = 1$, Y_o is equal to C_i . Moreover, the sum $(R_{ct} + Z_d)$ corresponds to the faradaic or reaction impedance. The structure of this sum reflects the fact that the faradaic current, i.e., the overall rate of the electrode reaction, is controlled by

two impedance elements in series connection, accounting for diffusion and reaction kinetics.²⁰

The charge-transfer resistance is directly related to the electron-transfer reaction of the probe molecules at the gold surface. Both in presence of the PMETAC brush or in its absence (electrode covered only with the initial SAM) the electron-transfer reaction takes place at bare spots or pinhole sites, i.e., at the uncovered electrode surface. Consequently, the fractional coverage of the monolayer of thiol initiator is the main factor that determines the absolute value of the measured charge-transfer resistance, particularly in the absence of a strong brush collapse that could further decrease the rate constant, as indicated above. However, with the electrode covered by the initial SAM alone the low-frequency region of the impedance spectra corresponds to semi-infinite diffusion in the electrolyte, while in the presence of the brush this spectral region is related to a finite-length diffusion of the electroactive probe inside the brush. This shows again that impedance measurements can sense in a distinctive way the effect of thermally induced transitions on both electron-transfer and diffusion processes occurring in the polymer brush.⁶

When the electron-transfer rate of the redox couple is not markedly diminished by a collapse transition, the global reaction rate within the polymeric environment is generally controlled by ion transport or, at least, exhibits a mixed control. This might resemble the condition set by a polymer brush conformation described as a compressed state in contrast to a fully collapsed state.²¹ On the other hand, when the electron transfer at the substrate is markedly inhibited due to a strong collapse of the brush, impedance data may not be able to resolve both contributions separately. Indeed, the low-frequency mass-transfer region may not be observed because the reaction is under kinetic control over the entire frequency range. In the literature, a strong conformational transition that collapses the structure was discussed related to either the presence of a very high concentration of counterions exhibiting ion-pairing interactions with the polymer chain (e.g., 1 M NaClO₄) or for a polymer film relatively thick before collapsing.⁵

Typical results of the good agreement obtained between theory and experiment are shown in terms of both Nyquist and Bode plots in Figures 10 and 11 for a selected temperature $T = 35\text{ }^{\circ}\text{C}$ in the two electrolytic solutions.

Interestingly, fit parameter R_{ct} is inversely proportional to the real electrode area (eq 3) unlike fit parameter B which is independent of the electrode area. Since B is used together with the d (previously measured) to calculate D (eq 4), variations in

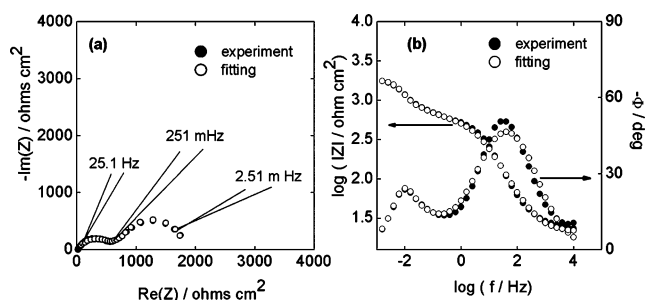


Figure 10. Nyquist (a) and Bode (b) plots of impedance data for Au electrodes coated with a PMETAC brush in 0.1 M NaCl containing 1 mM $\text{K}_3[\text{Fe}(\text{CN})_6]/\text{K}_4[\text{Fe}(\text{CN})_6]$ (1:1) mixture at $T = 35\text{ }^{\circ}\text{C}$. Experimental data (●) and fit results (○) according to eq 5

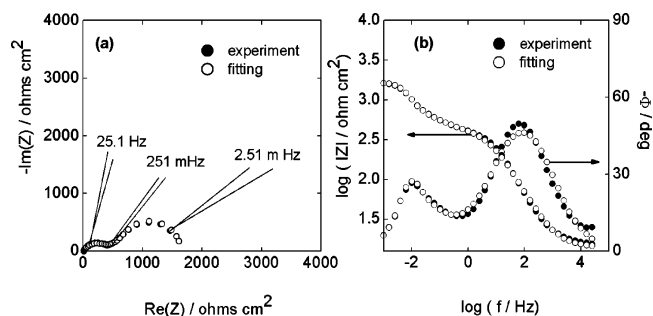


Figure 11. Nyquist (a) and Bode (b) plots of impedance data for Au electrodes coated with PMETAC in 0.1 M NaClO₄ containing 1 mM $\text{K}_3[\text{Fe}(\text{CN})_6]/\text{K}_4[\text{Fe}(\text{CN})_6]$ (1:1) mixture at $T = 35\text{ }^{\circ}\text{C}$. Experimental data (●) and fit results (○) according to eq 5.

the latter cannot be ascribed to changes in the active area according to the working conditions.¹⁵

Assuming, as usual, that the transfer coefficients $\alpha_a = \alpha_c = 0.5$ for both anodic and cathodic reactions²² and remembering that the applied dc potential corresponds to the formal potential of the redox couple ($C_O^{\text{dc}} = C_R^{\text{dc}} = C$) results in $k_c = k_a = k$ and eq 3 reduces to

$$\frac{T}{R_{ct}} = \frac{A_e F^2 C}{R} k \quad (6)$$

Since k obeys the Arrhenius equation from the slope of the linear plot $\ln(T/R_{ct})$ vs $1/T$ the activation energy can be calculated.²³

T variations of k and D in terms of Arrhenius plots are shown in Figures 12 and 13 within the studied $5\text{--}45\text{ }^{\circ}\text{C}$ temperature range in the two electrolytic solutions.

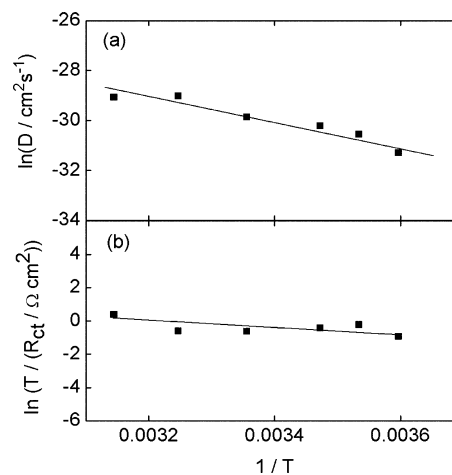


Figure 12. Arrhenius plots for the diffusion coefficient (a) and the kinetic constant (b) for Au electrodes coated with a PMETAC brush in 0.1 M NaCl containing 1 mM $\text{K}_3[\text{Fe}(\text{CN})_6]/\text{K}_4[\text{Fe}(\text{CN})_6]$ (1:1) mixture. Data derived from impedance fit parameters (R_{ct} and B) and the brush acoustic thickness (d_{QCM}).

Activation energy for the diffusional process in Cl^- solution (Figure 13a) is ca. 38 kJ mol^{-1} while for the electron transfer it is ca. 19 kJ mol^{-1} (Figure 12b).

In NaClO₄ solution (Figure 13b) it can be observed that the electron transfer requires different activation energies whether the process occurs below or above a certain threshold temperature that was interpreted as the glass transition

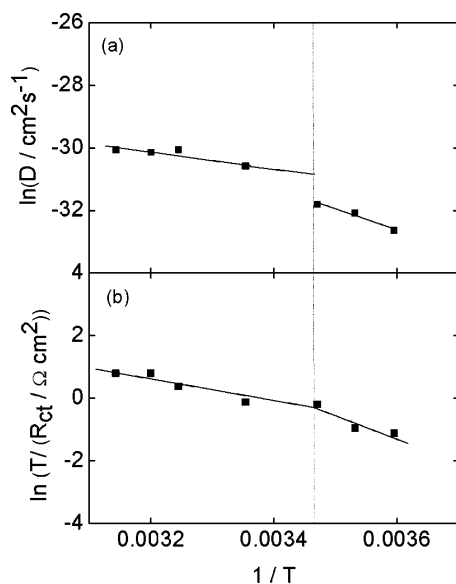


Figure 13. Arrhenius plots for the diffusion coefficient (a) and the kinetic constant (b) for PMETAC-modified electrodes in 0.1 M NaClO_4 containing 1 mM $\text{K}_3[\text{Fe}(\text{CN})_6]/\text{K}_4[\text{Fe}(\text{CN})_6]$ (1:1) mixture. Data derived from impedance fit parameters (R_{ct} and B) and the brush acoustic thickness (d_{QCM}).

temperature of the brush T_g^8 assuming a glassy state for the PMETAC brushes bearing ClO_4^- counterions below this temperature. Activation energy values calculated from the experimental data are ca. 60 and 29 kJ/mol for temperature values below and above this $T_g \cong 17^\circ\text{C}$, respectively. These results indicate that the activation energy for the electron transfer taking place within the brush in a “glassy” state is twice the activation energy in the “rubbery” state. Moreover, around the T_g the measured diffusion coefficient of the redox probe inside the brush decreases up to ca. 3 times, from 4.12×10^{-14} to $1.48 \times 10^{-14} \text{cm}^2 \text{s}^{-1}$, associated with the thermal transition into the glassy region. The final value for D observed at 5°C is $1.26 \times 10^{-14} \text{cm}^2 \text{s}^{-1}$, being $2.56 \times 10^{-14} \text{cm}^2 \text{s}^{-1}$ at the same temperature for the brushes in NaCl . The activation energy for the diffusional process in ClO_4^- solution (Figure 13a) is ca. 24 kJ mol^{-1} for temperatures above T_g that result in a value lower than the value obtained in Cl^- solution. However, below T_g the activation energy for the diffusional process in ClO_4^- solution becomes much larger and close to 60 kJ mol^{-1} . Clearly, both reaction steps result independently inhibited by the thermal transition. Interestingly, polyelectrolyte multilayers modifying Au electrodes and in contact with a solution of 0.5 M NaClO_4 and 1 mM $\text{K}_4\text{Fe}(\text{CN})_6$ resulted in a diffusion coefficient for the redox probe inside the polymeric assembly that follows the Arrhenius law, and the activation energy was estimated as 61 kJ mol^{-1} .²⁴

When PMETAC brushes collapse by ion pairing with ClO_4^- ions, they show very compact stiff structures with less entrapped water and so markedly different from the same brushes whose collapse is driven by pure Coulombic screening. This has been quantitatively discussed above and confirmed by means of indentation experiments with atomic force microscopy and also more qualitatively by QCM-D.³ Since water plays a role of plasticizer in the glassy state, increasing the fluidity of the material and lowering the T_g , this could explain why in our measurements only the brushes in contact with a ClO_4^- solution exhibit a detectable thermal transition in the studied

temperature range.²⁵ Moreover, this transition can be reversibly changed back to the original state reversing the medium temperature beyond T_g .

At this point it is perhaps worth mentioning that additional QCM-D experiments were performed that allowed confirmation that the brush thickness remained independent of the electrolyte temperature within the working temperature range (data not shown). It is clear that a decrease in temperature below the glass transition limit does not lead to a further collapse of the structure, at least in the temperature range studied. Regardless of its precise origin, the thermal behavior of the PMETAC brush in ClO_4^- solution is characterized by a morphological nanostructural transition at a well-defined temperature that has a direct impact on the mass transport through the brush and on the electron transfer at the substrate. Clearly, a switchable thermocontrolled electrode activity induced specific counterions represents an interesting case of thermally controlled electrode interface with surface states becoming less active or inactive for the electrochemical process of the redox species (i.e., $[\text{Fe}(\text{CN})_6]^{3-/4-}$ anions). In a separate work we reported recently⁸ glass transition temperature measurements in PMETAC brushes in ClO_4^- solutions using impedance spectroscopy as a novel method for the determination of T_g . Likewise, the highly restricted mass transport inside the brush below T_g results in an adaptive surface selective for ionic species having catalytic or pharmaceutical activity.²⁶ The glass transition is associated with a change in the local degrees of freedom. At the T_g the spacing and free internal volume available for molecular motions achieve minimum values. Thus, it is reasonable to expect that a glass transition may lead to increased reorganization energy for the redox species during the electron jump²⁷ or, put in other words, may lead to increased activation energy for the electron transfer. Moreover, the usual model describing the influence of the solvent–polymer interaction on diffusion coefficients is the free volume model. This model proposes that mass transport is regulated by the re-distribution of the polymer free volume within the solvent²⁸ and predicts a decrease in transport of a solute (+solvent) into a polymer matrix with a decrease in solvent–polymer (and solute–polymer) interactions.

Noteworthy, temperature effects are different according to the counterion in the supporting electrolyte. While the activation energies are markedly different for the diffusion and electron-transfer steps in chloride solution, they are practically the same for these two steps in perchlorate solution, even when the thermal transition takes place.

4. CONCLUSION

We have shown that impedance spectroscopy (EIS) can be used to resolve separately the thermal effects of diffusion and electron-transfer steps of an electrochemical reaction taking place at a brush-modified electrode. Additionally, a link between these effects and the structural transitions of the polymer brush has been proposed. Results lead to the conclusion that the electron-transfer step exhibits lower activation energy when the grafted brush suffers a collapse transition resulting from purely electrostatic screening of charges, using NaCl to trigger collapse than when the collapse transition is promoted by ion-pairing interactions, induced by the counterion ClO_4^- . Charge screening collapse induced by NaCl reduces water content only to a lesser degree, and polymer chains remain more viscous as we can interpret from the changes in dissipation. Increasing temperature inside the

brush leads to increased chain mobility, which offers the probe more possibilities for diffusing through free space between the chains. However, in the case of the brushes collapsed with ClO_4^- counterions, the lower water content and restricted chain mobility hinder diffusion pathways for the probe. This causes the mobility of the probe to be significantly lower at temperatures below 17 °C than for the PMETAC brush in NaCl under equal conditions. Only when the temperature exceeds 17 °C, chain mobility is largely increased and the probe can find a more favorable pathway for diffusion. This thermal transition of the polymer layer has a strong impact on the mass transport through the brush as well as the electron transfer at the substrate. The activation energy for the electron transfer in the “glassy” state is twice as large as the activation energy in the “rubbery” state. The experimental evidence presented in this work shows the full potential of a specific counterion to modify/tune the rates of electrochemical reactions taking place at electrode surfaces modified with polyelectrolyte brushes, something that is essential for improving technological applications that rely on molecule–surface interactions, such as designing new electrocatalysts for use in synthesis and power-generation/energy-storage applications. For instance, stimulus-triggered ionic transport enhancements would greatly improve the versatility/adaptability of electrochemical functions within polymer brush layers, including electrochemiluminescence for light-emitting diodes, electrochromic thin films, and impedance-based sensors. Another interesting example is the development of synthetic strategies for producing interfacial architectures based on polyelectrolyte brushes to facilitate proton transport. Extensive research conducted during recent years revealed that polyelectrolyte brush films show great promise in that both polyelectrolyte nanostructures and local solvation dynamics can be tuned and optimized to facilitate ion transport.^{29–31} However, our understanding of solvent and ion dynamics in highly conductive and crowded polymeric environments is scarce.³² These studies combining electrochemical impedance and QCM studies provide further insight into the delicate interplay between ion diffusion, electron-transfer energy barriers, and polymer/ion hydration within the macromolecular environment. We consider that these results are important in unraveling the functional richness of polymer brushes and establishing new concepts of material design to attain functional polymer thin films with controllable interfacial transport properties.

AUTHOR INFORMATION

Corresponding Authors

*Tel.: +54-221-425-7430. Fax: +54-221-425-4642. E-mail: gervasi@inifta.unlp.edu.ar. Homepage: <http://softmatter.quimica.unlp.edu.ar>.

*Tel.: +54-221-425-7430. Fax: +54-221-425-4642. E-mail: azzaroni@inifta.unlp.edu.ar. Homepage: <http://softmatter.quimica.unlp.edu.ar>.

Notes

The authors declare no competing financial interest.

ACKNOWLEDGMENTS

This work was financially supported by the Marie Curie project “Transport Studies on Polymer Based Nanodevices and Assemblies for Delivery and Sensing” (TRASNADE; Grant 247656). C.A.G. gratefully acknowledges ANPCyT-Argentina through Grant PICT No. 2008-1902 and the Comisión de

Investigaciones Científicas y Técnicas de Buenos Aires (CICBA) for his position as a member of the Carrera del Investigador Científico. O.A. is a CONICET fellow and acknowledges financial support from the Alexander von Humboldt Stiftung (Germany), Fundación Petruzza, the Max Planck Society (Germany), and ANPCyT-Argentina (Grants PICT-PRH 163/08, PICT-2010-2554). S.E.M. acknowledges support from the Spanish Ministry of Science and Innovation (Grant MAT2010-18995).

REFERENCES

- (1) Azzaroni, O. Polymer Brushes Here, There and Everywhere: Recent Advances in Their Practical Applications and Emerging Opportunities in Multiple Research Fields. *J. Polym. Sci., Part A: Polym. Chem.* **2012**, *50*, 3225–3258.
- (2) Azzaroni, O.; Brown, A. A.; Cheng, N.; Wei, A.; Jonas, A. M.; Huck, W. T. S. Synthesis of Gold Nanoparticles Inside Polyelectrolyte Brushes. *J. Mater. Chem.* **2007**, *17*, 3433–3439.
- (3) Azzaroni, O.; Moya, S.; Farhan, T.; Brown, A. A.; Huck, W. T. S. Switching the Properties of Polyelectrolyte Brushes via Hydrophobic Collapse. *Macromolecules* **2005**, *38*, 10192–10199.
- (4) Iturri Ramos, J. J.; Moya, S. E. Water Content of Hydrated Polymer Brushes Measured by an in Situ Combination of a Quartz Crystal Microbalance with Dissipation Monitoring and Spectroscopic Ellipsometry. *Macromol. Rapid Commun.* **2011**, *32*, 1972–1978.
- (5) Zhou, F.; Hu, H. Y.; Yu, B.; Osborne, V. L.; Huck, W. T. S.; Liu, W. M. Probing the Responsive Behavior of Polyelectrolyte Brushes Using Electrochemical Impedance Spectroscopy. *Anal. Chem.* **2007**, *79*, 176–182.
- (6) Azzaroni, O.; Gervasi, C. A. Characterization of Responsive Polymer Brushes at Solid/Liquid Interfaces by Electrochemical Impedance Spectroscopy In *Functional Polymer Films, Characterization and Applications*, 1st ed.; Knoll, W., Advincula, R. C., Eds.; Wiley-VCH Verlag: Weinheim, Germany, 2011; Vol. 2, Chapter 26, pp 809–830.
- (7) Rodríguez Presa, M. J.; Gassa, L. M.; Azzaroni, O.; Gervasi, C. A. Estimating Diffusion Coefficients of Probe Molecules into Polyelectrolyte Brushes by Electrochemical Impedance Spectroscopy. *Anal. Chem.* **2009**, *81*, 7936–7943.
- (8) Alonso-García, T.; Rodríguez-Presa, M. J.; Gervasi, C. A.; Moya, S.; Azzaroni, O. Electrochemical Determination of the Glass Transition Temperature of Thin Polyelectrolyte Brushes at Solid–Liquid Interfaces by Impedance Spectroscopy. *Anal. Chem.* **2013**, *85*, 6561–6565.
- (9) Choi, E.-Y.; Azzaroni, O.; Cheng, N.; Zhou, F.; Kelby, T.; Huck, W. T. S. H. Electrochemical Characteristics of Polyelectrolyte Brushes with Electroactive Counterions. *Langmuir* **2007**, *23*, 10389–10394.
- (10) Sauerbrey, G. Verwendung von Schwingquarzen zur Wägung dünner Schichten und zur Mikrowägung. *Z. Phys.* **1959**, *155*, 206–222.
- (11) Domack, A.; Prucker, O.; Rühle, J.; Johannsmann, D. Swelling of a polymer brush probed with a quartz crystal resonator. *Phys. Rev. E: Stat. Phys., Plasmas, Fluids, Relat. Interdiscip. Top.* **1997**, *56*, 680–689.
- (12) Voinova, M. V.; Rodahl, M.; Jonson, M.; Kasemo, B. Viscoelastic acoustic response of layered polymer films at fluid-solid interfaces. *Phys. Scr.* **1999**, *59*, 391–396.
- (13) Daimon, M.; Masumura, A. Measurement of the refractive index of distilled water from the near-infrared region to the ultraviolet region. *Appl. Opt.* **2007**, *46*, 3811–3820.
- (14) Moya, S.; Azzaroni, O.; Farhan, T.; Osborne, V. L.; Huck, W. T. S. Locking and Unlocking of Polymer Brushes: Towards the Fabrication of Nanoactuators. *Angew. Chem., Int. Ed.* **2005**, *44*, 4578–4581.
- (15) Ramos, J. J. I. Assembly and Physico-Chemical Characterization of Supramolecular Polyelectrolyte Nanostructures. Ph.D. Thesis, Doctor Europeus, San Sebastián, Spain, 2011.
- (16) Seshadri, K.; Wilson, A. M.; Guiseppe-Elie, A.; Allara, D. L. Toward Controlled Area Electrode Assemblies: Selective Blocking of Gold Electrode Defects with Polymethylene Nanocrystals. *Langmuir* **1999**, *15*, 742–749.

(17) Finklea, H. O.; Snider, D. A.; Fedyk, J.; Sabatani, E.; Gafni, Y.; Rubinstein, I. Characterization of octadecanethiol-coated gold electrodes as microarray electrodes by cyclic voltammetry and ac impedance spectroscopy. *Langmuir* **1993**, *9*, 3660–3667.

(18) Alonso-García, T.; Gervasi, C. A.; Rodríguez-Presa, M. J.; Irigoyen-Otamendi, J.; Moya, S. E.; Azzaroni, O. Molecular Transport in Thin Thermo-Responsive Poly(*N*-isopropylacrylamide) Brushes with Varying Grafting Density. *J. Phys. Chem. C* **2012**, *116*, 13944–13953.

(19) Qu, D. The Study of the Proton Diffusion Process in the Porous MnO₂ Electrode. *Electrochim. Acta* **2004**, *49*, 657–665.

(20) Freger, V.; Bason, S. Characterization of Ion Transport in Thin Films Using Electrochemical Impedance Spectroscopy: I. Principles and Theory. *J. Membr. Sci.* **2007**, *302*, 1–9.

(21) Gao, X.; Kučerka, N.; Nieh, M.-P.; Katsaras, J.; Zhu, S.; Brash, J. L.; Sheardown, H. Chain Conformation of a New Class of PEG-Based Thermoresponsive Polymer Brushes Grafted on Silicon as Determined by Neutron Reflectometry. *Langmuir* **2009**, *25*, 10271–10278.

(22) Limat, M.; El Roustom, B.; Jotterand, H.; Fóti, G.; Comninellis, C. Electrochemical and Morphological Characterization of Gold Nanoparticles Deposited on Boron-Doped Diamond Electrode. *Electrochim. Acta* **2009**, *54*, 2410–2416.

(23) Imre, Á.W.; Schönhoff, M.; Cramer, C. A Conductivity Study and Calorimetric Analysis of Dried Poly(sodium 4-styrene sulfonate)/Poly(diallyldimethylammonium chloride) Polyelectrolyte Complexes. *J. Chem. Phys.* **2008**, *128*, No. 134905.

(24) Silva, T. H.; Garcia-Morales, V.; Moura, C.; Manzanares, J. A.; Silva, F. Electrochemical Impedance Spectroscopy of Polyelectrolyte Multilayer Modified Gold Electrodes: Influence of Supporting Electrolyte and Temperature. *Langmuir* **2005**, *21*, 7461–7467.

(25) Yeo, S. C.; Eisenberg, A. Effect of Ion Placement and Structure on Properties of Plasticized Polyelectrolytes. *J. Macromol. Sci., Part B: Phys.* **1977**, *13*, 441–484.

(26) Spruijt, E.; Choi, E.-Y.; Huck, W. T. S. Reversible Electrochemical Switching of Polyelectrolyte Brush Surface Energy Using Electroactive Counterions. *Langmuir* **2008**, *24*, 11253–11260.

(27) Eckermann, A. L.; Feld, D. J.; Shaw, J. A.; Meade, T. J. Electrochemistry of Redox-Active Self Assembled Monolayers. *Coord. Chem. Rev.* **2010**, *254*, 1769–1802.

(28) Pickup, S.; Blum, F. D. Self-diffusion of Toluene in Polystyrene Solutions. *Macromolecules* **1989**, *2* × *2*, 3961–3968.

(29) Yameen, B.; Kaltbeitzel, A.; Langner, A.; Duran, H.; Müller, F.; Gösele, U.; Azzaroni, O.; Knoll, W. Facile Large-Scale Fabrication of Proton Conducting Channels. *J. Am. Chem. Soc.* **2008**, *130*, 13140–13144.

(30) Yameen, B.; Kaltbeitzel, A.; Langer, A.; Müller, F.; Gösele, F.; Knoll, W.; Azzaroni, O. Highly Proton-Conducting Self-Humidifying Microchannels Generated by Copolymer Brushes on a Scaffold. *Angew. Chem., Int. Ed.* **2009**, *48*, 3124–3128.

(31) Yameen, B.; Kaltbeitzel, A.; Glasser, G.; Langer, A.; Müller, F.; Gösele, F.; Knoll, W.; Azzaroni, O. Hybrid Polymer-Silicon Proton Conducting Membranes via a Pore-Filling Surface-Initiated Polymerization Approach. *ACS Appl. Mater. Interfaces* **2010**, *2*, 279–287.

(32) Wang, S.; Jing, B.; Zhu, Y. Molecule Motion at Polymer Brush Interfaces from Single-Molecule Experimental Perspectives. *J. Polym. Sci., Part B: Polym. Phys.* **2014**, DOI: 10.1002/polb.23414.